의학석사 학위논문

중증근무력증 환자에서 차세대 시퀀싱기법을 이용한 질병활성도에 따른 혈액전사체 연구

Blood transcriptome analysis in myasthenia gravis patients according to the disease activity

2015년 2월

서울대학교 대학원
의학과 뇌신경과학 전공
박 기 홍

중증근무력증 환자에서 차세대 시퀀싱기법을 이용한 질병활성도에 따른 혈액전사체 연구

Blood transcriptome analysis in myasthenia gravis patients according to the disease activity

지도교수 이광우

이 논문을 뇌신경과학 의학석사 학위논문으로 제출함

2015년 2월

서울대학교 대학원

의학과 뇌신경과학 전공

박기홍

박기홍의 의학석사 학위논문을 인준함.

2015년 2월

위원장	박성혜	(인)
부위원장	이광우	(인)
위원	홍윤호	(인)

Abstract

Blood transcriptome analysis in myasthenia gravis patients according to the disease activity

Kee Hong Park

Graduate Program of Neuroscience

Department of Medicine

The Graduate School

Seoul National University

Background : Myasthenia gravis (MG) is an autoimmune disease affecting components of muscle membrane at the neuromuscular junction. Remission of the disease can be achieved by using immunosuppressants, but little is known about their mechanisms without biomarkers to monitor the response to treatment. With advent of next generation sequencing, it became possible to analyze whole transcriptome with RNA sequencing technique. We investigated transcriptome of peripheral blood mononuclear cells obtained from MG patients to identify molecular signatures of disease activity.

Methods : Quantitative global mRNA sequencing analysis of peripheral blood mononuclear cells (PBMC) was performed in 5 patients on active state and 5 patients on remission state. Active

state was defined as de novo state or refractory symptoms despite of optimal treatment. Gene expression profiles were compared between two groups by using Cuffdiff and DESeq. Gene expression pathway analysis was done with DAVID Bioinformatics Resources and Ingenuity Pathway Analysis in the set of differentially expressed genes (DEG).

Results : By using Cuffdiff, we identified 98 differentially expressed transcripts at greater than two-fold change with raw p value < 0.05 (63 up-regulated, 35 down-regulated genes in remission group), whereas DESeq revealed 292 genes (165 up-regulated and 127 down-regulated). Among them, 28 genes were commonly observed as DEGs in both of analyses (23 up-regulated and 5 down-regulated). Top 5 genes of up-regulated genes were PFKFB3, CTSG, RAB20, S100P and BEX1, while down-regulated genes were S100B, OAS1, SLC25A20, MAP3K7CL and LINC00861. On pathway analysis, cell motion and cell migration clusters were differentially enriched between two groups. These clusters included ICAM1, CCL3, S100P and GAB2. Apoptosis pathway was also differentially enriched, and it contained NFKBIA, ZC3H12A, TNFAIP3 and PPP1R15A.

Conclusion : This study reveals the transcripts and functional clusterings associated with MG disease activity. Among the DEGs, S100B and CXCR3 were down-regulated in remission group and these may have potential to be biomarkers to indicate the disease activity. Cell migration and apoptosis pathways were differentially

enriched between active and remission groups. Based on these results, further studies will be needed to understand the pathophysiology of MG and to find the therapeutic target.

Key words : myasthenia gravis, RNA-seq, transcriptome

Student number : 2010-21854

Contents

List of Tables and Figures

List of Abbreviations

myasthenia gravies, MG

peripheral blood mononuclear cells, PBMC

differentially expressed genes, DEG

neuromuscular junction, NMJ

intravenous-immunoglobulin, IVIG

Acetylcholine receptor antibody, AChR Ab

muscle-specific tyrosine kinase, MuSK

lipoprotein receptor-related protein 4, LRP4

next generation sequencing, NGS

Fragment Per Kilobase of exon per Million fragments mapped, FPKM

Myasthenia Gravis Foundation of America, MGFA

gene ontology, GO

Database for Annotation, Visualization and Integrated Discovery, DAVID

Ingenuity Pathway Analysis, IPA

multidimensional scaling, MDS

experimental autoimmune myasthenia gravis, EAMG

genome-wide association studies, GWAS

early onset myasthenia gravis, EAMG

Introduction

Myasthenia gravis (MG) is an autoimmune disease caused by autoantibody attack against components of muscle membrane at the neuromuscular junction(NMJ), which manifests as fatigue and fluctuating weakness (1). Based on the etiology, immunotherapies are tried and their treatment responses are effective in most of the patients. Traditionally, corticosteroids and non-steroidal agents such as azathioprine, mycophenolate mofetil, cyclophosphamide, cyclosporine, tacrolimus and rituximab are used for the long term immunosuppressant therapy, whereas intravenous-immunoglobulin (IVIG) and plasmapheresis are tried for the short-term disease control (2). Moreover, new biological agents are tried for the specific molecule targeted therapy (3). However, the pathomechanism of the disease has not been fully understood yet, and there is little information about which molecule or pathway is related to the treatment. And there has been no effective monitoring modality about treatment response, so far. Therefore, it is necessary to develop therapeutic biomarkers to investigate the disease mechanism, to monitor individual patients, and to develop the new drug by establishing therapeutic target.

Biomarker development in MG have been restricted to diagnostic biomarkers up to now (4).Acetylcholine receptor antibody (AChR Ab)

was found in about 85% of MG patients, whereas muscle-specific tyrosine kinase (MuSK)antibody and low-density lipoprotein receptor-related protein 4 (LRP4) antibody were found in 5% and 2% each (5). Anti-agrin antibody was newly established in other seronegative MG patients (6). Therefore, the understanding of diagnostic biomarker about MG has been broadened, but there are limitations of these molecules in therapeutic decision and monitoring. So the demand for alternative biomarker is increasing.

Recently, transcriptomic research techniques were introduced to assess the immunologic disease and its biomarkers (7). With development of high-throughput molecular technologies, genomic approaches became available. Genomic approaches can be divided into DNA and RNA analysis, but transcriptomic approach which is handling RNA is more appropriate to study immune-mediated diseases, because it reflects dynamic activity of immune system. Microarray has been routinely used for the transcriptome study. Amplified RNA was labeled with oligonucleotide probes, and RNA abundance was imaged according to its signal intensity (8). However, with development ofnext generation sequencing (NGS), RNA seq technique emerged as an alternative method with some advantages upon microarray, such as high accuracy, revealing the precise boundaries of transcripts, and yielding information about exon junctions, and so on (9).

There have been some transcriptome studies to investigate

immunologic pathomechanism of MG (10 - 14). However, there have been no studies regarding therapeutic response in MG. So we divided MG patients according to the disease activity, the active group and the remission group. Target organ for transcriptome study of MG can be thymus or neuromuscularjunction, but these tissues are difficult to assess in vivo. Rather, immune cells in the blood are easy to obtain, and these may reflect actual immune status of autoimmune disease. Furthermore, investigating changes of transcriptome profile can be more suitable for monitoring of individual patients. By investigating the difference of mRNA profile in PBMCs between two groups, this study can provide information about therapeutic biomarker in MG.

Materials and Methods

Patients

The MG patients were recruited from the neurology department of Seoul National University Boramae Hospital from September 2013 to April 2014. Patients were divided into active group and remission group (complete stable remission, pharmacologic remission, minimal manifestation), and each group included 5 patients. Active group included patients with de novo MG or patients with refractory MG despite optimal treatment, and activity of disease was graded by Myasthenia Gravis Foundation of America Clinical Classification (15). Complete stable remission was defined as no symptoms or signs of MG without treatment for at least 1 year, pharmacologic remission as no symptoms or signs of MG with immunosuppressive treatment, and minimal manifestation as no symptoms of functional limitations from MG with some weakness on examination. In active group, there were 2 MGFA class I, 1 MGFA class IIa and 2 MGFA class IIIa patients. In remission group, there were 2 minimal manifestation and 3 pharmacological remission patients. Two patients provided samples at both active state and remission state. Written informed consent was obtained from the patients.

PBMC isolation and RNA purification

For the PBMC isolation, the Lymphoprep™ was used according to the manufacturer's protocol. Ready-made medium was placed in the tube, and then blood sample diluted with saline with 1:1 was added. After centrifuging 20 minutes at 600g, sedimented PBMCs were harvested.

With isolated PBMC sample, RNA purification was done with RNeasy® Mini kit. Cell pellet was mixed with RLT buffer and 70% ethanol. The lysate was then loaded to the RNeasy Mini spin column, so the RNA binded and contaminants were washed away. DNase was added to remove residual DNA efficiently.

RNA-Seq Experiment

The mRNA-Seq sample was obtained using Illumina®TruSeq™RNA Sample Preparation Kit. Purifying the poly-A containing mRNA molecules with poly-T oligo-attached magnetic beads was the first step, followed by thermal mRNA fragmentation. The RNA fragments were then transcribed into first strand cDNA using reverse transcriptase and random primers. The cDNA was synthesized to second strand cDNA using DNA Polymerase I and RNaseH. After end repair process, single 'A' bases were added to the fragments, and then adapters were ligated, preparing cDNA for hybridization onto a flow cell. Finally, the products were purified and enriched with PCR to create the cDNA library. (Macrogen, Korea, http://www.macrogen.c

o.kr)

Aligning RNA-Seq reads and abundance estimation

Fragmented cDNAs were aligned using TopHat v.2.0.11 (16). It aligned reads to human genomes (UCSC version hg19) using Bowtie 2.1.0 algorithm (17). Abundance of aligned reads were estimated by Cufflinks v.2.1.1 (18). It accepted aligned reads and assembled the alignments into a simple and clear set of transcripts. Then RNA-seq fragment counts were measured by the unit of Fragment Per Kilobase of exon per Million fragments mapped (FPKM) (19).

Statistical Analysis

The values of log2 (FPKM+1) were calculated and these were normalized by quantile normalization. P values were obtained by t-test between the active group and the remission group and fold changes were calculated with the mean log2 (FPKM+1) values, gene by gene.

Pathway analysis using DAVID and IPA

For gene ontology (GO) analysis of the transcritptome, functional

clustering was done by the Database for Annotation, Visualization and Integrated Discovery (DAVID v.6.7). DEG list was uploaded via the web interface, (http://david.abcc.ncifcrf.gov) and the background was designated as *Homo sapiens* (20). Annotation clusters were selected according to the threshold enrichment score 1.3. Enrichment score 1.3 is equivalent to non-log scale 0.05. Another functional analysis was done by Ingenuity Pathway Analysis (IPA) software (licensed use of Ingenuity® Systems, www. Ingenuity.com). To identify functions which are expected to be increased or decreased, downstream analysis was conducted by uploading statistically significant DEGs from DESeq.

Results

RNA Seq data analysis

Overall, there were 48385 transcripts and we excluded any transcripts with 0 FPKM value. There were 37745 transcripts with 0 FPKM, leaving 10640 transcripts to be analyzed.

Prior to DEG analysis, the data from the 10640 filtered genes were used for multidimensional scaling (MDS) analysis (Figure 1). This analysis demonstrated that MG samples were roughly differentiated according to the disease activity along the first plot dimension.

Differentially expressed genes (DEG)

Gene expression was compared by independent t-test with FPKM value. 98 genes were significantly different between two groups (fold change $\geq$ 2, p value $<$ 0.05). Among them, 63 genes were up-regulated and 35 genes were down-regulated in remission state (Supplemental Table S1, S2). Top 5 genes of up-regulated genes were LTF, DEFA4, ELANE, AZU1 and CAMP, while down-regulated genes were S100B, LINC00861, PTGDS, OAS1 and OAS2 (Table 1). Volcano plot shows the differential expression levels of genes between active and remission group (Figure 2A). Heat map for

hierarchical clustering was shown in Figure 2B with unsupervised clustering method. Second column of remission group represents the patient whose MDS data was closely related to active group (Figure 2B).

DESeq, another tool for DEG analysis, was used to compare the results with Cuffdiff's. More DEGs were derived with DESeq analysis, i.e. 165 up-regulated genes and 127 down-regulated genes in active group (Supplemental Table S3, S4). Top 5 genes of up-regulated genes were PFKFB3, CTSG, HIST1H1D, RAB20 and C10orf55, while down-regulated genes were TAS2R4, KRT74, SPTSSB, CLDN24 and DIP2A (Table 2).

To enhance robustness of analysis, we investigated the commonly detected genes both in Cuffdiff and DESeq analysis. Twenty-eight genes were commonly found (23 up-regulated and 5 down-regulated genes, Table 3) and Venn diagram was shown in Figure 3. Top 5 genes of up-regulated genes were PFKFB3, CTSG, RAB20, S100P and BEX1, while down-regulated genes were S100B, OAS1, SLC25A20, MAP3K7CL and LINC00861.

Paired samples which were included in both groups were analyzed separately with FPKM values. There were 18 up-regulated genes (fold change $\geq$ 2, p value $<$ 0.05), but there were no down-regulated genes (Table 4). All the up-regulated genes except TPGS1 were commonly found in the DEG list with whole study samples.

Pathway analysis using DAVID and IPA

DAVID analysis revealed the enriched gene ontology categories with commonly up-regulated genes, and the result was shown in Table 5. Annotation cluster 1 included cell motion, cell migration, localization of cell and cell motility categories, and ICAM1, CCL3, S100P and GAB2 were belonged to this cluster. Annotation cluster 2 contained apoptosis, programmed cell death, cell death and death categories, and NFKBIA, ZC3H12A, TNFAIP3 and PPP1R15A belonged to this cluster. Number of commonly down-regulated genes was not sufficient to analyze.

Downstream effect analysis using IPA was shown in Figure 4. Top 5 categories were hematologic system development and function, immune cell trafficking, cellular movement, inflammatory response and cell-to-cell signaling and interaction pathways. Most of the functional annotations related to these categories were down-regulated in active group. Top 5 down-regulated functional annotations (activation z-score $\leq$ -2) were chemotaxis of cells, cell movement of monocytes, chemotaxis of monocytes, differentiation of blood cells and chemotaxis of phagocytes (data not shown).

Table 1. Top 5 list of up-regulated and down-regulated genes in remission group with Cuffdiff analysis

Gene symbol	Raw *P* value	R/A fc[a]	Description
Up-regulated			
LTF	0.01434	10.171	lactotransferrin
DEFA4	0.01186	10.111	defensin, alpha 4, corticostatin
ELANE	0.00609	9.6151	elastase, neutrophil expressed
AZU1	0.00674	8.6584	azurocidin 1
CAMP	0.01912	7.9296	cathelicidin antimicrobial peptide
Down-regulated			
S100B	0.0244	-3.3166	S100 calcium binding protein B
LINC00861	0.01407	-2.8543	long intergenic non-protein coding RNA 861
PTGDS	0.03568	-2.77	prostaglandin D2 synthase 21kDa (brain)
OAS1	0.00892	-2.7556	2′-5′-oligoadenylate synthetase 1, 40/46kDa
OAS2	0.03202	-2.5589	2′-5′-oligoadenylate synthetase 2, 69/71kDa

[a]Fold change ratio of expression in active group to remission group

Table 2. Top 5 list of up-regulated and down-regulated genes in remission group with DESeq analysis

Gene symbol	Raw *P* value	R/A log2 fc[a]	Description
Up-regulated			
PFKFB3	1.13E-06	-1.965336085	6-phosphofructo-2-kinase/fructose -2,6-biphosphatase 3
CTSG	5.67E-06	-1.87927551	cathepsin G
HIST1H1D	8.42E-06	-1.854834675	histone cluster 1, H1d
RAB20	7.42E-08	-1.760501814	RAB20, member RAS oncogene family
C10orf55	2.29E-05	-1.71010185	chromosome 10 open reading frame 55
Down-regulated			
TAS2R4	3.25E-06	1.93119111	taste receptor, type 2, member 4
KRT74	1.22E-06	1.91868424	keratin 74
SPTSSB	4.89E-06	1.840058846	serine palmitoyltransferase, small subunit B
CLDN24	1.12E-05	1.833322418	claudin 24
DIP2A	3.53E-06	1.676968833	DIP2 disco-interacting protein 2 homolog A (Drosophila)

[a]Fold change ratio of expression in active group to remission group

Table 3. List of commonly detected genes both in Cuffdiff and DESeq analysis

Gene symbol	Description
Up-regulated	
PFKFB3	6-phosphofructo-2-kinase/fructose-2,6-biphosphatase 3
CTSG	cathepsin G
RAB20	RAB20, member RAS oncogene family
S100P	S100 calcium binding protein P
BEX1	brain expressed, X-linked 1
PTX3	pentraxin 3, long
CCL3	chemokine (C-C motif) ligand 3
UHRF1BP1L	UHRF1 binding protein 1-like
TNFAIP3	tumor necrosis factor, alpha-induced protein 3
RELL1	RELT-like 1
ICAM1	intercellular adhesion molecule 1
NFKBIA	nuclear factor of kappa light polypeptide gene enhancer in B-cells inhibitor, alpha
PPP1R15A	protein phosphatase 1, regulatory subunit 15A
CD69	CD69 molecule
RGS1	regulator of G-protein signaling 1
SLC7A5	solute carrier family 7 (amino acid transporter light chain, L system), member 5
B3GNT5	UDP-GlcNAc:betaGal beta-1,3-N-acetylglucosaminyltransferase 5
LTF	lactotransferrin
FAM46A	family with sequence similarity 46, member A
FUT4	fucosyltransferase 4 (alpha (1,3) fucosyltransferase, myeloid-specific)
ZC3H12A	zinc finger CCCH-type containing 12A
HIF1A-AS2	HIF1A antisense RNA 2
GAB2	GRB2-associated binding protein 2
Down-regulated	
S100B	S100 calcium binding protein B
OAS1	2′-5′-oligoadenylate synthetase 1, 40/46kDa
SLC25A20	solute carrier family 25 (carnitine/acylcarnitinetranslocase), member 20
MAP3K7CL	MAP3K7 C-terminal like
LINC00861	long intergenic non-protein coding RNA 861

Table 4. List of up-regulated genes in paired samples' remission group

Gene symbol	Raw *P* value	R/A fc[a]	Description
DEFA4	5.02E-06	3.67418	defensin, alpha 4, corticostatin
PRTN3	0.015388	3.56934	proteinase 3
AZU1	0.021954	3.55711	azurocidin 1
ELANE	0.009671	3.54981	elastase, neutrophil expressed
LTF	0.016599	3.44459	lactotransferrin
CAMP	0.032415	3.38222	cathelicidin antimicrobial peptide
CTSG	0.026329	3.2908	cathepsin G
OLFM4	0.010717	3.20382	olfactomedin 4
CEACAM8	0.019415	3.18208	carcinoembryonic antigen-related cell adhesion molecule 8
LCN2	0.009297	3.1791	lipocalin 2
CEACAM6	0.031206	3.00076	carcinoembryonic antigen-related cell adhesion molecule 6 (non-specific cross reacting antigen)
RNASE3	0.005035	3.00003	ribonuclease, RNase A family, 3
PGLYRP1	0.017687	2.97606	peptidoglycan recognition protein 1
TPGS1	0.036323	2.84443	tubulin polyglutamylase complex subunit 1
S100P	0.034514	2.72674	S100 calcium binding protein P
SLPI	0.036938	2.5616	secretory leukocyte peptidase inhibitor
NDUFS1	0.02878	2.33752	NADH dehydrogenase (ubiquinone) Fe-S protein 1, 75kDa (NADH-coenzyme Q reductase)
PRPF38A	0.021574	2.03714	pre-mRNA processing factor 38A

[a]Fold change ratio of expression in active group to remission group

Table 5. Functional annotation analysis using DAVID

Term	*P* Value	Genes
Annotation Cluster 1, Enrichment Score: 1.4384248684673653		
cell motion (GO:0006928)	0.017131	ICAM1, CCL3, S100P, GAB2
cell migration (GO:0016477)	0.041231	ICAM1, S100P, GAB2
localization of cell (GO:0051674)	0.049962	ICAM1, S100P, GAB2
cell motility (GO:0048870)	0.049962	ICAM1, S100P, GAB2
Annotation Cluster 2, Enrichment Score: 1.3933537552043205		
apoptosis (GO:0006915)	0.031854	NFKBIA, ZC3H12A, TNFAIP3, PPP1R15A
programmed cell death (GO:0012501)	0.03309	NFKBIA, ZC3H12A, TNFAIP3, PPP1R15A
cell death (GO:0008219)	0.049903	NFKBIA, ZC3H12A, TNFAIP3, PPP1R15A
death (GO:0016265)	0.050769	NFKBIA, ZC3H12A, TNFAIP3, PPP1R15A

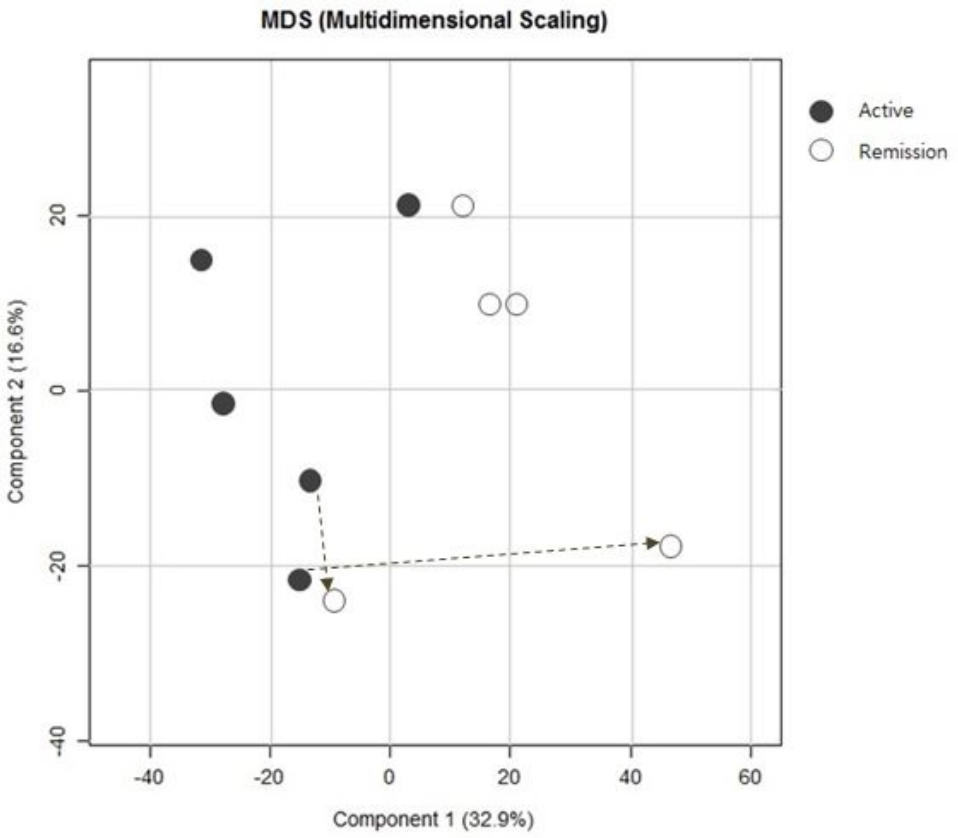

Figure 1. Multidimensional Scaling plot of the gene profiles. This visualizes the similarity between individual samples. The first plot dimension roughly corresponds to disease activity and the second plot to patient differences. Paired samples are linked by dotted arrows.

(A)

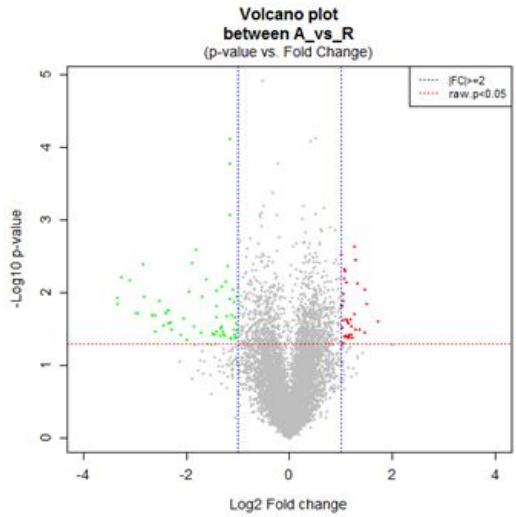

(B)

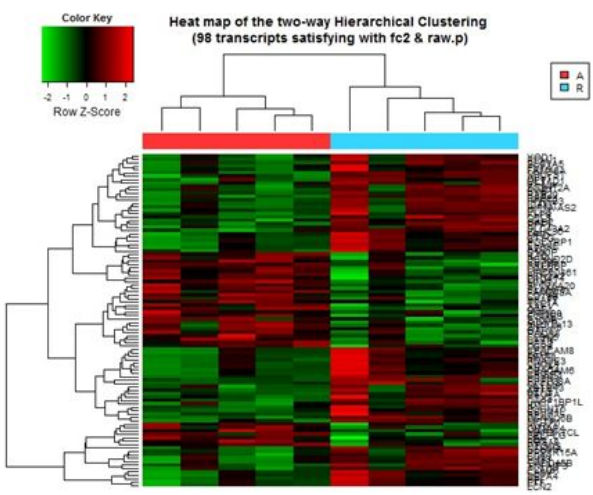

Figure 2. Differentially expressed genes. (A) Volcano plot showing the differential expression levels of genes between active and remission group. Significant up-regulated and down-regulated genes are shown in red and green dots. (B) Heat map for unsupervised hierarchical clustering based on differentially expressed genes (fold change $\geq$ 2, p value $<$ 0.05).

(A)

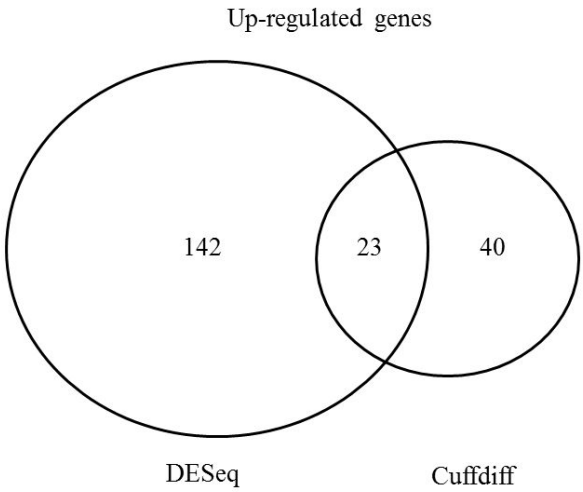

(B)

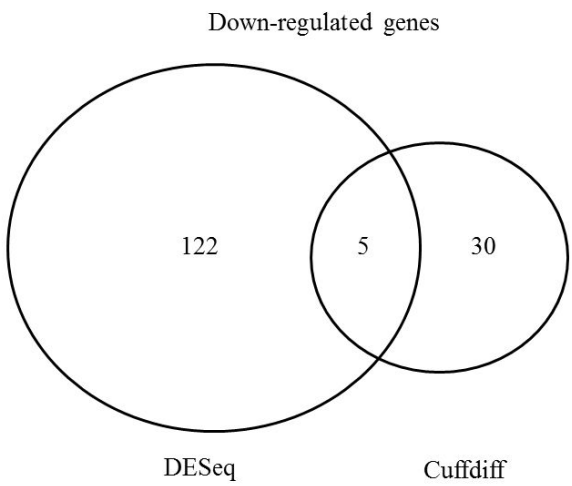

Figure 3. Venn diagram of DEGs from DESeq and Cuffdiff. (A) Up-regulated genes in active group. (B) Down-regulated genes in active group. There were 5 common up-regulated genes and 23 down-regulated genes detected.

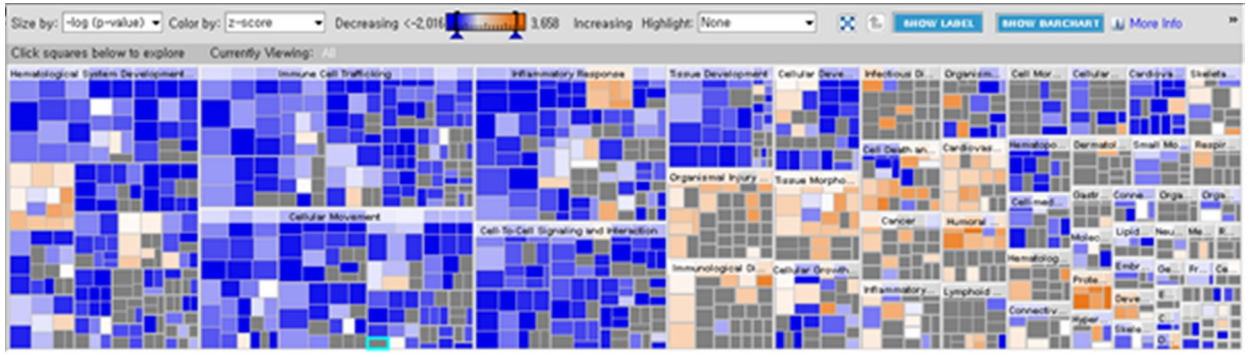

Figure 4. Downstream analysis using IPA. Major boxes represent a category of related functions and each individual small boxes represent a particular biological function or disease. Orange color indicates increased predicted effects, and blue color indicates decreased effects. Intensity of each color indicate the degree of absolute Z-score. Top 5 categories were hematologic system development and function, immune cell trafficking, cellular movement, inflammatory response and cell-to-cell signaling and interaction pathways. Most of the functional annotations were down-regulated in active group.

Discussion

In this report, we describe the transcriptome of peripheral blood mononuclear cells in MG patients. Extensive research of references was done with DEG lists. Some genes were previously reported related with MG, and need further discussion. Pathway analysis using DAVID and IPA revealed several pathways which may be related to the disease activity of MG.

S100B, which is the most up-regulated gene in active group, is a ligand of the receptor for advanced glycation end products (RAGE). RAGE is a central signal transduction receptor mediating effects of S100-calgranulins on key cellular targets, including mononuclear phagocytes, lymphocytes and vascular endothelial cells, which indicates the relevance of RAGE to inflammatory disorders (21). In experimental autoimmune myasthenia gravis (EAMG), S100B level was significantly higher, and it increased the number of AChR Ab secreting splenocytes, which was reversed by COX-2 inhibitor (22). Mean value of S100B of MG was higher than normal controls, but it was not statistically significant (23). In multiple sclerosis which is another autoimmune-mediated neurologic disease, S100B was up-regulated in mouse model (21) and decreased along immunosuppressive treatment in MS patients (24), which showed the potential for the therapeutic marker.

CTTN encodes cortactin which is associated with NMJ development and needed for the formation of AChR cluster. Recently, antibody against cortactin was reported in 19.7% of seronegative MG and 4.8% of seropositive MG patients (25). The role of cortactin and its antibody should be investigated further.

LTF, which was down-regulated in active group, encodes an iron-binding glycoprotein of the transferrin family. This prevent pro-inflammatory pathway activation, and reduces inflammatory responses via up-regulating the expression of Th2, Th17 and regulatory T cells (26). It is known that imbalance between Th1 cell's cytokines and Th2 cell's cytokines may play a key role in the development of MG (27). Decreased LTF may be a factor of imbalanced T cell inflammatory system.

ABL1 is a non-receptor tyrosine kinase characterized by unique carboxy-terminal actin-binding domains, and this is critical mediator of postsynaptic assembly at the NMJ via providing a specific tyrosine kinase activity downstream of the MuSK receptor that is required for agrin-induced AChR clustering (28). Clustering increases density of AChR at neuromuscular junction and also induces a higher stability of AChRs (29). Down-regulated ABL1 in active group may play a role in efficient NMJ signal conduction.

It is known that B cell activation plays a role in MG because of evidences of polyclonal activation in MG, and B cell activating factor (BAFF) is considered as a therapeutic target (30). Three studies have

shown that higher BAFF level in MG patients compared to control subjects, but it was not associated with disease severity (31 - 33). One study has shown that BAFF level was significantly decreased in MG patients under immunosuppresive therapy in comparison with untreated population (31). In our study, TNFSF13B, whch encodes BAFF was not differentially expressed. Genetic predisposition was investigated using genome-wide association studies (GWAS) in another study, and PTPN22 and TNIP1 were associated with early onset MG (EAMG) (34). TNIP1 is TNFAIP3-interacting protein 1, and is thought to be involved in NF-κB signaling pathway. TNIP1 gene was not differentially expressed in this study, but TNFAIP3 was down-regulated in active group. Variants of TNFAIP3 was reported in GWAS of systemic lupus erythematosus and rheumatoid arthritis, but was not reported in MG patients of Hellenic population (35). TNFAIP3 interferes inflammation by inhibiting NF-κB signaling pathway, and its abundance may have affected the disease activity, and may be affected by ethnicity.

Epigenetic pattern may be a link between environment and genetic background, and the concept of epigenetics has been extended to microRNA (34). miRNA microarray study revealed that MiR-320a was down-regulated in MG patients (27). MiR-320a is also involved in NF-κB signaling pathway and this regulates inflammatory cytokine expression. These results indicate that further study should be focused on this pathway.

Among the significant annotation clusters in DAVID analysis, first annotation cluster includes cell motion, cell migration, localization of cell and cell motility. There are some reports that these pathways are related to MG pathophysiology. CXCL13 and CCL21 were overexpressed in hyperplastic thymus (13,36) and CXCR5 was overexpressed on T cells of MG patients (37). However, all the related genes in this study were down-regulated in active group, in contrast to previous studies. This tendency was verified in downstream analysis of IPA. Among the top 5 pathways, there were immune cell trafficking, cellular movement, inflammatory response and cell-to-cell signaling and interaction pathways, and all of them were down-regulated in active group. We could make some assumptions about this phenomenon. First, most previous studies compared between MG patients and healthy population, but accomplishment of remission state might not be related to these pathways. Second, it could be due to discrepancy regarding target organ (such as thymus or neuromuscular junction) and blood cells. In previous report about active rheumatoid arthritis, chemokine receptor profile of PMBCs was increased with treatment, and the authors explained it as a compensation mechanism (38). Lastly, expression of chemokines might be influenced by study group's demographic characteristics. CXCL13 chemokine was differentially expressed according to the onset class and clinical class (39). It was significantly increased in young-age patient group (age < 40 years) compared to control group, but on the

contrary, it was decreased in old-age patient group (age ≥ 40 years). All of the patients of our study were older than 40 years, and this might influenced the result.

Meanwhile, chemokine receptor CXCR3 was up-regulated in active group, and previous report noted that CXCR3 mRNA level was increased in both thymus and muscle of MG patients (40). Follow up study showed that inhibiting CXCR3 with CXCR3 antagonist led to suppression of EAMG (41). These previous studies and our data indicate that CXCR3 could be a potential therapeutic target.

Annotation cluster 2 contained apoptosis, programmed cell death, cell death and death categories. Immunosuppressive agents are mainstay of treatment for MG and their mechanisms are related with these pathways. Corticosteroids induce T lymphocyte apoptosis, and other agents also inhibit cell proliferation (42). All of the remission group patients received prednisolone, and three patients also received tacrolimus, another T cell apoptosis inducer (43).

This is the first study investigating blood transcriptome according to the disease activity in MG. Some genes may have potential to be therapeutic biomarker candidate, and the role of cell migration pathway and apoptosis in immunosuppressive treatment in MG should be further investigated. However, there are some limitations to acknowledge. Treatment modality was not homogenized, and the pathway or individual genes might be affected by the drug type. Study sample size was relatively small. To compensate these

limitations, we used two different software packages to increase the robustness of DEG analysis. A number of analysis tools have been developed, but there is no consensus about the best practices yet (44). Cuffdiff determines differential expression using t-test from FPKM values based on beta negative binomial model (18), while DESeq uses exact test based on negative binomial model (45). These two methods were used in our study, and commonly detected genes in both analyses were used for the pathway analysis. Furthermore, RT-PCR will be needed to validate more accurate RNA abundance value in candidate genes.

Conclusion

This study reveals the transcripts and functional clustering associated with MG disease activity. Among the DEGs, S100B may have potential to be a biomarker to indicate the disease activity. CXCR3 was up-regulated in active group, and it could be a therapeutic target in MG. Cell migration and apoptosis pathways were differentially enriched between active and remission groups. Based on these results, further studies will be needed to understand the pathophysiology of MG and to find the therapeutic target.

References

1. Berrih-Aknin S, Le Panse R. Myasthenia gravis: a comprehensive review of immune dysregulation and etiological mechanisms. J Autoimmun. 2014 Aug;52:90 - 100.
2. Jayam Trouth A, Dabi A, Solieman N, Kurukumbi M, Kalyanam J. Myasthenia gravis: a review. Autoimmune Dis. 2012 Jan;2012:874680.
3. Dalakas MC. Novel future therapeutic options in myasthenia gravis. Autoimmun Rev. 2013 Jul;12(9):936 - 41.
4. Kaminski HJ, Kusner LL, Wolfe GI, Aban I, Minisman G, Conwit R, et al. Biomarker development for myasthenia gravis. Ann N Y Acad Sci. 2012 Dec;1275:101 - 6.
5. Berrih-Aknin S, Frenkian-Cuvelier M, Eymard B. Diagnostic and clinical classification of autoimmune myasthenia gravis. J Autoimmun. 2014;48-49:143 - 8.
6. Gasperi C, Melms A, Schoser B, Zhang Y, Meltoranta J, Risson V, et al. Anti-agrin autoantibodies in myasthenia gravis. Neurology. 2014 Jun 3;82(22):1976 - 83.
7. Chaussabel D, Pascual V, Banchereau J. Assessing the human immune system through blood transcriptomics. BMC Biol. 2010 Jan;8:84.
8. Mirnics K, Pevsner J. Progress in the use of microarray technology to study the neurobiology of disease. 2004;7(5):434 -

9.

9. Sánchez-Pla A, Reverter F, Ruíz de Villa MC, Comabella M. Transcriptomics: mRNA and alternative splicing. J Neuroimmunol. 2012 Jul 15;248(1-2):23 - 31.

10. Le Panse R, Cizeron-Clairac G, Bismuth J, Berrih-Aknin S. Microarrays reveal distinct gene signatures in the thymus of seropositive and seronegative myasthenia gravis patients and the role of CC chemokine ligand 21 in thymic hyperplasia. J Immunol. 2006 Dec 1;177(11):7868 - 79.

11. Gradolatto A, Nazzal D, Truffault F, Bismuth J, Fadel E, Foti M, et al. Both Treg cells and Tconv cells are defective in the Myasthenia gravis thymus: roles of IL-17 and TNF-α. J Autoimmun. 2014 Aug;52:53 - 63.

12. Feferman T, Aricha R, Menon R, Souroujon MC, Berrih-Aknin S, Fuchs S. DNA microarray in search of new drug targets for myasthenia gravis. Ann N Y Acad Sci. 2007 Jun;1107:111 - 7.

13. Meraouna A, Cizeron-Clairac G, Panse R Le, Bismuth J, Truffault F, Tallaksen C, et al. The chemokine CXCL13 is a key molecule in autoimmune myasthenia gravis. Blood. 2006 Jul 15;108(2):432 - 40.

14. Poea-Guyon S, Christadoss P, Le Panse R, Guyon T, De Baets M, Wakkach A, et al. Effects of Cytokines on Acetylcholine Receptor Expression: Implications for Myasthenia Gravis. J Immunol. 2005 May 5;174(10):5941 - 9.

15. Jaretzki A, Barohn R, Ernstoff R. Myasthenia gravis

Recommendations for clinical research standards. Neurology. 2000;55:16 – 23.

16. Trapnell C, Pachter L, Salzberg SL. TopHat: discovering splice junctions with RNA-Seq. Bioinformatics. 2009 May 1;25(9):1105 – 11.

17. Langmead B, Trapnell C, Pop M, Salzberg SL. Ultrafast and memory-efficient alignment of short DNA sequences to the human genome. Genome Biol. 2009 Jan;10(3):R25.

18. Trapnell C, Williams B a, Pertea G, Mortazavi A, Kwan G, van Baren MJ, et al. Transcript assembly and quantification by RNA-Seq reveals unannotated transcripts and isoform switching during cell differentiation. Nat Biotechnol. 2010 May;28(5):511 – 5.

19. Twine N a, Janitz K, Wilkins MR, Janitz M. Whole transcriptome sequencing reveals gene expression and splicing differences in brain regions affected by Alzheimer's disease. PLoS One. 2011 Jan;6(1):e16266.

20. Huang DW, Sherman BT, Lempicki R a. Systematic and integrative analysis of large gene lists using DAVID bioinformatics resources. Nat Protoc. 2009 Jan;4(1):44 – 57.

21. Biophysics C, Hospital FA. Suppression of experimental autoimmune encephalomyelitis by selective blockade of encephalitogenic T-cell infiltration of the central nervous system. Nat Med. 2003;9(3):287 – 93.

22. Mu L, Zhang Y, Sun B, Wang J, Xie X, Li N, et al. Activation

of the receptor for advanced glycation end products (RAGE) exacerbates experimental autoimmune myasthenia gravis symptoms. Clin Immunol. 2011 Oct;141(1):36 - 48.

23. Moser B, Bekos C, Zimprich F, Nickl S, Klepetko W, Ankersmit J. The receptor for advanced glycation endproducts and its ligands in patients with myasthenia gravis. Biochem Biophys Res Commun. 2012 Mar 30;420(1):96 - 101.

24. Bartosik-Psujek H, Psujek M, Jaworski J, Stelmasiak Z. Total tau and S100b proteins in different types of multiple sclerosis and during immunosuppressive treatment with mitoxantrone. Acta Neurol Scand. 2011 Apr;123(4):252 - 6.

25. Gallardo E, Martínez-Hernández E, Titulaer MJ, Huijbers MG, Martínez MA, Ramos A, et al. Cortactin autoantibodies in myasthenia gravis. Autoimmun Rev. 2014 Sep 3;13(10):1003 - 7.

26. Siqueiros-Cendón T, Arévalo-Gallegos S, Iglesias-Figueroa BF, García-Montoya IA, Salazar-Martínez J, Rascón-Cruz Q. Immunomodulatory effects of lactoferrin. Acta Pharmacol Sin. 2014 May;35(5):557 - 66.

27. Cheng Z, Qiu S, Jiang L, Zhang A, Bao W, Liu P, et al. MiR-320a is downregulated in patients with myasthenia gravis and modulates inflammatory cytokines production by targeting mitogen-activated protein kinase 1. J Clin Immunol. 2013 Apr;33(3):567 - 76.

28. Finn AJ, Feng G, Pendergast AM. Postsynaptic requirement for Abl kinases in assembly of the neuromuscular junction. Nat

Neurosci. 2003 Jul;6(7):717 - 23.

29. Zong Y, Jin R. Structural mechanisms of the agrin-LRP4-MuSK signaling pathway in neuromuscular junction differentiation. Cell Mol Life Sci. 2013 Sep;70(17):3077 - 88.

30. Berrih-Aknin S, Ragheb S, Le Panse R, Lisak RP. Ectopic germinal centers, BAFF and anti-B-cell therapy in myasthenia gravis. Autoimmun Rev. 2013 Jul;12(9):885 - 93.

31. Scuderi F, Alboini PE, Bartoccioni E, Evoli A. BAFF serum levels in myasthenia gravis: effects of therapy. J Neurol. 2011 Dec;258(12):2284 - 5.

32. Kim JY, Yang Y, Moon J-S, Lee EY, So SH, Lee H-S, et al. Serum BAFF expression in patients with myasthenia gravis. J Neuroimmunol. 2008 Aug 13;199(1-2):151 - 4.

33. Stavern G Van, Gonzales F, Simon K. A Potential Role for B-Cell Activating Factor in the Pathogenesis of Autoimmune Myasthenia Gravis. 2015;65(10):1358 - 62.

34. Avidan N, Le Panse R, Berrih-Aknin S, Miller A. Genetic basis of myasthenia gravis - a comprehensive review. J Autoimmun. 2014 Aug;52:146 - 53.

35. Zagoriti Z, Georgitsi M, Giannakopoulou O, Ntellos F, Tzartos SJ, Patrinos GP, et al. Genetics of myasthenia gravis: a case-control association study in the Hellenic population. Clin Dev Immunol. 2012 Jan;2012:484919.

36. Berrih-Aknin S, Ruhlmann N, Bismuth J, Cizeron-Clairac G, Zelman E, Shachar I, et al. CCL21 overexpressed on lymphatic

vessels drives thymic hyperplasia in myasthenia. Ann Neurol. 2009 Oct;66(4):521 - 31.

37. Saito R, Onodera H, Tago H, Suzuki Y, Shimizu M, Matsumura Y, et al. Altered expression of chemokine receptor CXCR5 on T cells of myasthenia gravis patients. J Neuroimmunol. 2005 Dec 30;170(1-2):172 - 8.

38. Nissinen R, Leirisalo-Repo M, Peltomaa R, Palosuo T, Vaarala O. Cytokine and chemokine receptor profile of peripheral blood mononuclear cells during treatment with infliximab in patients with active rheumatoid arthritis. Ann Rheum Dis. 2004 Jun;63(6):681 - 7.

39. Shiao Y-M, Lee C-C, Hsu Y-H, Huang S-F, Lin C-Y, Li L-H, et al. Ectopic and high CXCL13 chemokine expression in myasthenia gravis with thymic lymphoid hyperplasia. J Neuroimmunol. 2010 Apr 15;221(1-2):101 - 6.

40. Feferman T, Maiti PK, Berrih-Aknin S, Bismuth J, Bidault J, Fuchs S, et al. Overexpression of IFN-Induced Protein 10 and Its Receptor CXCR3 in Myasthenia Gravis. J Immunol. 2005 Apr 20;174(9):5324 - 31.

41. Feferman T, Aricha R, Mizrachi K, Geron E, Alon R, Souroujon MC, et al. Suppression of experimental autoimmune myasthenia gravis by inhibiting the signaling between IFN-gamma inducible protein 10 (IP-10) and its receptor CXCR3. J Neuroimmunol. 2009 Apr 30;209(1-2):87 - 95.

42. Sanders DB, Evoli A. Immunosuppressive therapies in

myasthenia gravis. Autoimmunity. 2010 Aug;43(5-6):428 - 35.

43. Ponseti JM, Gamez J, Azem J, López-Cano M, Vilallonga R, Armengol M. Tacrolimus for myasthenia gravis: a clinical study of 212 patients. Ann N Y Acad Sci. 2008 Jan;1132:254 - 63.

44. Seyednasrollah F, Laiho A, Elo LL. Comparison of software packages for detecting differential expression in RNA-seq studies. Brief Bioinform. 2015 Dec 2;16:59 - 70.

45. Anders S, Huber W. Differential expression analysis for sequence count data. Genome Biol. 2010 Jan;11(10):R106.

Table S1. List of up-regulated genes in remission group with Cuffdiff analysis

Gene symbol	Raw *P* value	R/A fc[a]	Description
LTF	0.01434	10.171	lactotransferrin
DEFA4	0.01186	10.111	defensin, alpha 4, corticostatin
ELANE	0.00609	9.6151	elastase, neutrophil expressed
AZU1	0.00674	8.6584	azurocidin 1
CAMP	0.01912	7.9296	cathelicidin antimicrobial peptide
LCN2	0.01926	7.757	lipocalin 2
CTSG	0.00404	7.181	cathepsin G
PRTN3	0.01144	7.0652	proteinase 3
PGLYRP1	0.02032	6.3741	peptidoglycan recognition protein 1
MMP8	0.03368	6.1277	matrix metallopeptidase 8 (neutrophil collagenase)
BPI	0.02044	6.1198	bactericidal/permeability-increasing protein
PFKFB3	0.01277	5.7464	6-phosphofructo-2-kinase/fructose-2,6-biphosphatase 3
CEACAM8	0.02823	5.4994	carcinoembryonic antigen-related cell adhesion molecule 8
MPO	0.01927	5.3247	myeloperoxidase
CEACAM6	0.01766	5.2006	carcinoembryonic antigen-related cell adhesion molecule 6 (non-specific cross reacting antigen)
CHI3L1	0.0264	5.115	chitinase 3-like 1 (cartilage glycoprotein-39)
CRISP3	0.01709	5.0704	cysteine-rich secretory protein 3
RNASE3	0.02518	4.9346	ribonuclease, RNase A family, 3
SLPI	0.03195	4.9049	secretory leukocyte peptidase inhibitor
ANXA3	0.03723	4.3495	annexin A3
S100P	0.02262	4.1479	S100 calcium binding protein P
OLFM4	0.04379	3.9769	olfactomedin 4
RAB21	0.00974	3.8669	RAB21, member RAS oncogene family
RAB20	0.00388	3.7354	RAB20, member RAS oncogene family
TNFAIP3	0.02914	3.6049	tumor necrosis factor, alpha-induced protein 3
NDUFS1	0.00254	3.5043	NADH dehydrogenase (ubiquinone) Fe-S protein 1, 75kDa
ID1	0.03487	3.277	inhibitor of DNA binding 1, dominant negative

			helix-loop-helix protein
CCL3	0.01139	3.2186	chemokine (C-C motif) ligand 3
UHRF1BP1L	0.00644	3.0718	UHRF1 binding protein 1-like
RGS1	0.04968	3.0039	regulator of G-protein signaling 1
01-Mar	0.03672	2.8354	membrane-associated ring finger (C3HC4) 1, E3 ubiquitin protein ligase
PRPF38A	0.03735	2.7403	pre-mRNA processing factor 38A
CD69	0.03383	2.6753	CD69 molecule
ICAM1	0.00923	2.6681	intercellular adhesion molecule 1
NFKBIA	0.01504	2.6654	nuclear factor of kappa light polypeptide gene enhancer in B-cells inhibitor, alpha
SLC7A5	0.02147	2.66	solute carrier family 7 (amino acid transporter light chain, L system), member 5
ATF3	0.03101	2.5344	activating transcription factor 3
ZC3H12A	0.03859	2.513	zinc finger CCCH-type containing 12A
GLT1D1	0.02903	2.5051	glycosyltransferase 1 domain containing 1
KLHL36	0.00831	2.4792	kelch-like family member 36
PTX3	0.0339	2.457	pentraxin 3, long
ZBTB43	0.03797	2.4294	zinc finger and BTB domain containing 43
KLF9	0.03916	2.3945	Kruppel-like factor 9
VEGFA	0.00703	2.3616	vascular endothelial growth factor A
PPP1R15A	0.02117	2.3248	protein phosphatase 1, regulatory subunit 15A
GAB2	0.00422	2.298	GRB2-associated binding protein 2
DENND6B	7.69E-05	2.2465	DENN/MADD domain containing 6B
MCTP1	0.00084	2.2285	multiple C2 domains, transmembrane 1
RPF1	0.00017	2.2246	ribosome production factor 1 homolog (S. cerevisiae)
RELL1	0.01222	2.2245	RELT-like 1
PIM3	0.04258	2.2074	pim-3 oncogene
BEX1	0.04103	2.1886	brain expressed, X-linked 1
GADD45B	0.02011	2.1652	growth arrest and DNA-damage-inducible, beta
ABL1	0.00914	2.1428	c-abl oncogene 1, non-receptor tyrosine kinase
SLC43A2	0.03185	2.1246	solute carrier family 43 (amino acid system L transporter), member 2
FUT4	0.01324	2.122	fucosyltransferase 4 (alpha (1,3) fucosyltransferase, myeloid-specific)
PLAUR	0.02165	2.0877	plasminogen activator, urokinase receptor

PLK3	0.04137	2.0756	polo-like kinase 3
FAM46A	0.03789	2.0732	family with sequence similarity 46, member A
YOD1	0.0263	2.0596	YOD1 deubiquitinase
B3GNT5	0.04088	2.0563	UDP-GlcNAc:betaGal beta-1,3-N-acetylglucosaminyltransferase 5
CCRN4L	0.01148	2.0302	CCR4 carbon catabolite repression 4-like (S. cerevisiae)
HIF1A-AS2	0.03342	2.0255	HIF1A antisense RNA 2

[a]Fold change ratio of expression in remission group to active group

Table S2. List of down-regulated genes in remission group with Cuffdiff analysis

Gene symbol	Raw *P* value	R/A fc[a]	Description
S100B	0.0244	-3.3166	S100 calcium binding protein B
LINC00861	0.01407	-2.8543	long intergenic non-protein coding RNA 861
PTGDS	0.03568	-2.77	prostaglandin D2 synthase 21kDa (brain)
OAS1	0.00892	-2.7556	2′-5′-oligoadenylate synthetase 1, 40/46kDa
OAS2	0.03202	-2.5589	2′-5′-oligoadenylate synthetase 2, 69/71kDa
CD79B	0.00732	-2.5048	CD79b molecule, immunoglobulin-associated beta
SLAMF6	0.00351	-2.4347	SLAM family member 6
PAQR8	0.0316	-2.4347	progestin and adipoQ receptor family member VIII
XAF1	0.01987	-2.4116	XIAP associated factor 1
SLC25A20	0.00229	-2.3937	solute carrier family 25 (carnitine/acylcarnitine translocase), member 20
LBH	0.04101	-2.325	limb bud and heart development
SELPLG	0.02942	-2.316	selectin P ligand
EOMES	0.03735	-2.2939	eomesodermin
HPS3	0.02279	-2.2744	Hermansky-Pudlak syndrome 3
ZNF146	0.04113	-2.2367	zinc finger protein 146
GIMAP4	0.03716	-2.2346	GTPase, IMAP family member 4
GAPT	0.03877	-2.2229	GRB2-binding adaptor protein, transmembrane
DENND2D	0.02647	-2.2182	DENN/MADD domain containing 2D
DCAF7	0.04079	-2.1823	DDB1 and CUL4 associated factor 7
MAP3K7CL	0.02432	-2.1704	MAP3K7 C-terminal like
CREBBP	0.023	-2.1634	CREB binding protein
TCL1A	0.04067	-2.1605	T-cell leukemia/lymphoma 1A
CD79B	0.00714	-2.1598	CD79b molecule, immunoglobulin-associated beta
CTTN	0.00497	-2.1285	cortactin
KLRK1	0.0385	-2.1187	killer cell lectin-like receptor subfamily K, member 1
RGS18	0.00632	-2.099	regulator of G-protein signaling 18
ZNF600	0.04054	-2.0987	zinc finger protein 600

IL16	0.00465	-2.0913	interleukin 16
CLDN5	0.01014	-2.079	claudin 5
LPCAT1	0.02353	-2.0743	lysophosphatidylcholine acyltransferase 1
BTN3A2	0.01278	-2.0655	butyrophilin, subfamily 3, member A2
LGR6	0.0487	-2.0561	leucine-rich repeat containing G protein-coupled receptor 6
METTL13	0.03015	-2.0432	methyltransferase like 13
FAM208A	0.01502	-2.0354	family with sequence similarity 208, member A
MMD	0.00296	-2.011	monocyte to macrophage differentiation-associated

[a]Fold change ratio of expression in remission group to active group

Table S3. List of up-regulated genes in remission group with DESeq analysis

Gene symbol	Raw *P* value	R/A log2 fc[a]	Description
PFKFB3	1.13E-06	1.965336085	6-phosphofructo-2-kinase/fructose -2,6-biphosphatase 3
CTSG	5.67E-06	1.87927551	cathepsin G
HIST1H1D	8.42E-06	1.854834675	histone cluster 1, H1d
RAB20	7.42E-08	1.760501814	RAB20, member RAS oncogene family
C10orf55	2.29E-05	1.71010185	chromosome 10 open reading frame 55
KCNK5	1.32E-05	1.701682832	potassium channel, subfamily K, member 5
ANKRD18A	1.79E-05	1.673033606	ankyrin repeat domain 18A
MPP5	1.11E-05	1.573259706	membrane protein, palmitoylated 5 (MAGUK p55 subfamily member 5)
SERPINB10	0.000162	1.540647914	serpin peptidase inhibitor, clade B (ovalbumin), member 10
HIST1H1E	0.000214	1.538783996	histone cluster 1, H1e
GPR84	4.04E-07	1.535046054	G protein-coupled receptor 84
SLC6A6	2.47E-05	1.511113074	solute carrier family 6 (neurotransmitter transporter), member 6
TEKT2	0.000273	1.510908277	tektin 2 (testicular)
S100P	0.000274	1.500070586	S100 calcium binding protein P
CILP2	0.000285	1.498692844	cartilage intermediate layer protein 2
PCOLCE2	0.000393	1.479418339	procollagen C-endopeptidase enhancer 2
PER1	0.000339	1.437796576	period circadian clock 1
07-Mar	0.000493	1.433318969	membrane-associated ring finger (C3HC4) 7, E3 ubiquitin protein ligase
MVB12B	0.000456	1.432467378	multivesicular body subunit 12B
BEX1	0.000496	1.428296752	brain expressed, X-linked 1
CFAP97	0.000373	1.421163544	UPF0501 protein KIAA1430 isoform 2
JUN	0.000728	1.396402775	jun proto-oncogene
PHF3	0.000329	1.389814645	PHD finger protein 3 isoform 3
MIR6750	0.000649	1.387318348	microRNA mir-6750
VPS11	7.93E-05	1.378565923	vacuolar protein sorting-associated

			protein 11 homolog isoform 2
CTDSP1	0.000369	1.367815722	CTD (carboxy-terminal domain, RNA polymerase II, polypeptide A) small phosphatase 1
HRH2	0.000195	1.363191538	histamine receptor H2
PTX3	0.000408	1.363029555	pentraxin 3, long
SEMA6B	0.000381	1.359254319	sema domain, transmembrane domain (TM), and cytoplasmic domain, (semaphorin) 6B
HIST1H4E	0.001107	1.355499459	histone cluster 1, H4e
ZNF331	0.001141	1.354940371	zinc finger protein 331
GRASP	0.000968	1.35448947	GRP1 (general receptor for phosphoinositides 1)-associated scaffold protein
FBN1	6.95E-05	1.350849015	fibrillin 1
DUSP10	4.27E-05	1.347751593	dual specificity phosphatase 10
CCL3	2.66E-05	1.347345592	chemokine (C-C motif) ligand 3
SLC2A5	0.000592	1.34320822	solute carrier family 2 (facilitated glucose/fructose transporter), member 5
PRDX3	0.001375	1.334562228	peroxiredoxin 3
HP	0.00151	1.321168214	haptoglobin
FOSB	0.001473	1.320974766	FBJ murine osteosarcoma viral oncogene homolog B
ASTL	0.001078	1.318731752	astacin-like metallo-endopeptidase (M12 family)
PTGES	0.001134	1.306423977	prostaglandin E synthase
ACSL1	0.000246	1.3015167	acyl-CoA synthetase long-chain family member 1
RNF144B	0.000178	1.299065328	ring finger protein 144B
UHRF1BP1L	0.001956	1.280905061	UHRF1 binding protein 1-like
TNFAIP3	0.002339	1.268412235	tumor necrosis factor, alpha-induced protein 3
HIPK1	0.000562	1.26748088	homeodomain interacting protein kinase 1
COPS8	0.001323	1.261809854	COP9 signalosome subunit 8
RELL1	2.71E-05	1.251916701	RELT-like 1
ICAM1	0.000122	1.244870634	intercellular adhesion molecule 1
NFKBIA	0.000327	1.242350674	nuclear factor of kappa light polypeptide gene enhancer in B-cells inhibitor, alpha
MCAM	0.002249	1.241362046	melanoma cell adhesion molecule
AEBP2	0.001252	1.241065423	AE binding protein 2

C17orf77	0.003217	1.225349736	chromosome 17 open reading frame 77
PPP1R15A	6.47E-05	1.223155335	protein phosphatase 1, regulatory subunit 15A
MIR6749	0.003094	1.217907633	microRNA mir-6749
NEDD9	0.003258	1.209113729	neural precursor cell expressed, developmentally down-regulated 9
C19orf77	0.001981	1.208863666	chromosome 19 open reading frame 77
ARHGAP24	0.001531	1.206777007	Rho GTPase activating protein 24
CD69	0.000445	1.206220044	CD69 molecule
MIR6883	0.003437	1.204125021	microRNA mir-6883
SPTA1	0.003135	1.203284674	spectrin, alpha, erythrocytic 1 (elliptocytosis 2)
ADRA2B	0.003846	1.201595839	adrenoceptor alpha 2B
EIF4G3	0.004059	1.199349369	eukaryotic translation initiation factor 4 gamma, 3
PRDM1	0.000356	1.197274459	PR domain containing 1, with ZNF domain
HNRNPH1	0.001075	1.195414721	heterogeneous nuclear ribonucleoprotein H1 (H)
TMUB1	0.002424	1.194093502	transmembrane and ubiquitin-like domain containing 1
SNORD98	0.001211	1.192872982	small nucleolar RNA, C/D box 98
FAM177A1	0.004174	1.189928144	family with sequence similarity 177, member A1
BCL3	0.000745	1.18927659	B-cell CLL/lymphoma 3
CKAP2L	0.003154	1.188388403	cytoskeleton associated protein 2-like
CDT1	8.34E-05	1.183848444	chromatin licensing and DNA replication factor 1
ADAR	0.000463	1.182077649	adenosine deaminase, RNA-specific
DUSP8	0.002938	1.180540357	dual specificity phosphatase 8
PELI1	0.001506	1.179603567	pellino E3 ubiquitin protein ligase 1
FAM209B	0.000159	1.178117648	family with sequence similarity 209, member B
APOA1	0.003539	1.176016574	apolipoprotein A-I
NSUN4	0.004505	1.17486119	NOP2/Sun domain family, member 4
TMEM39A	0.00468	1.173803453	transmembrane protein 39A
USP15	0.001364	1.171288597	ubiquitin specific peptidase 15
GAS2L3	0.00034	1.16594451	growth arrest-specific 2 like 3
CNTLN	0.000995	1.165138784	centlein, centrosomal protein
NFKB2	0.004853	1.163187945	nuclear factor of kappa light polypeptide

			gene enhancer in B-cells 2 (p49/p100)
DGCR11	4.94E-05	1.162321797	DiGeorge syndrome critical region gene 11 (non-protein coding)
NAMPT	0.001813	1.158666573	nicotinamide phosphoribosyltransferase
VRK2	0.004197	1.158179785	vaccinia related kinase 2
LOC101927472	0.00526	1.157023626	
IL8	0.005002	1.15332348	interleukin 8
ORM1	0.005805	1.151020753	orosomucoid 1
NCF2	0.006031	1.146166578	neutrophil cytosolic factor 2
TANK	0.006039	1.145982324	TRAF family member-associated NFKB activator
CXCL9	0.002103	1.143296699	chemokine (C-X-C motif) ligand 9
SNAI1	0.005126	1.139425853	snail family zinc finger 1
UBE4B	0.001069	1.138775277	ubiquitination factor E4B
RGS1	0.003242	1.133981726	regulator of G-protein signaling 1
TSC22D3	0.001006	1.133045415	TSC22 domain family, member 3
SSH2	0.00642	1.131325482	slingshot protein phosphatase 2
TAF5L	0.0003	1.127927278	TAF5-like RNA polymerase II, p300/CBP-associated factor (PCAF)-associated factor, 65kDa
CEP170	0.001282	1.122582416	centrosomal protein 170kDa
SLC7A5	0.001305	1.118141094	solute carrier family 7 (amino acid transporter light chain, L system), member 5
WWP2	0.000448	1.117265635	WW domain containing E3 ubiquitin protein ligase 2
SPTLC1	0.001556	1.1157581	serine palmitoyltransferase, long chain base subunit 1
SYNGR3	0.000597	1.11374075	synaptogyrin 3
HRH2	0.003752	1.111625033	histamine receptor H2
B3GNT5	0.001197	1.110612394	UDP-GlcNAc:betaGal beta-1,3-N-acetylglucosaminyltransferase 5
E2F7	0.005406	1.109987841	E2F transcription factor 7
HIF1A-AS1	0.000187	1.109180417	HIF1A antisense RNA 1
LTF	0.003923	1.108920234	lactotransferrin
ETNK1	0.006157	1.099834525	ethanolamine kinase 1
CEBPB-AS1	0.0004	1.097130112	
UTF1	0.006558	1.095213387	undifferentiated embryonic cell transcription factor 1
UBL5	0.008745	1.090821968	ubiquitin-like 5

FAM46A	0.000312	1.090154805	family with sequence similarity 46, member A
FUT4	0.000261	1.089282981	fucosyltransferase 4 (alpha (1,3) fucosyltransferase, myeloid-specific)
GMPR2	0.008054	1.088674963	guanosine monophosphate reductase 2
LOC102724153	0.000564	1.088276661	
HJURP	0.007031	1.087017802	Holliday junction recognition protein
NR4A2	0.008032	1.086731582	nuclear receptor subfamily 4, group A, member 2
YPEL5	0.000802	1.084759099	yippee-like 5 (Drosophila)
ZNF705E	0.004129	1.08425412	zinc finger protein 705E
SETMAR	0.009077	1.084069809	SET domain and mariner transposase fusion gene
CEBPE	0.008789	1.082339015	CCAAT/enhancer binding protein (C/EBP), epsilon
ZC3H12A	0.000912	1.08143687	zinc finger CCCH-type containing 12A
ANKRD22	0.000513	1.080891098	ankyrin repeat domain 22
CCRL2	0.008752	1.079592838	chemokine (C-C motif) receptor-like 2
HIF1A-AS2	0.000488	1.077275192	HIF1A antisense RNA 2
NFKBIZ	0.001669	1.075904164	nuclear factor of kappa light polypeptide gene enhancer in B-cells inhibitor, zeta
AMPD3	0.008695	1.074908908	adenosine monophosphate deaminase 3
PTPRJ	0.002968	1.071392703	protein tyrosine phosphatase, receptor type, J
GAB2	0.001904	1.070640622	GRB2-associated binding protein 2
GAL3ST2	0.010229	1.068507873	galactose-3-O-sulfotransferase 2
LRRFIP1	0.002797	1.068030016	leucine rich repeat (in FLII) interacting protein 1
TUBA1A	0.000202	1.064490896	tubulin, alpha 1a
CAMKK1	0.010715	1.063933447	calcium/calmodulin-dependent protein kinase kinase 1, alpha
RAP1A	0.005952	1.061977524	RAP1A, member of RAS oncogene family
BUB1B	0.004631	1.061682901	BUB1 mitotic checkpoint serine/threonine kinase B
KMT2E	0.004397	1.055755018	lysine (K)-specific methyltransferase 2E
CDK16	0.001052	1.054520948	cyclin-dependent kinase 16
FURIN	0.004151	1.054163531	furin preproprotein
GDAP2	0.000374	1.051306895	ganglioside induced differentiation associated protein 2
IL1B	0.005081	1.046490851	interleukin 1, beta
IFITM10	0.003924	1.040410243	interferon induced transmembrane protein 10

TP53INP2	0.003447	1.039029705	tumor protein p53 inducible nuclear protein 2
RNF217	0.001618	1.036160762	ring finger protein 217
TET2	0.001884	1.035030619	tet methylcytosine dioxygenase 2
DUSP1	0.000293	1.034849231	dual specificity phosphatase 1
MIR181A1HG	0.010185	1.033724145	MIR181A1 host gene (non-protein coding)
MXI1	0.001237	1.032362785	MAX interactor 1, dimerization protein
DCTN5	0.011267	1.031885565	dynactin 5 (p25)
TBC1D3P1-DHX40P1	0.009525	1.030435395	TBC1D3P1-DHX40P1 readthrough transcribed pseudogene
ELF2	0.000675	1.026216913	E74-like factor 2 (ets domain transcription factor)
LGALS3	0.001709	1.023561374	lectin, galactoside-binding, soluble, 3
SLC25A3	0.001671	1.023427626	solute carrier family 25 (mitochondrial carrier; phosphate carrier), member 3
GYPA	0.012259	1.019020585	glycophorin A (MNS blood group)
PIGA	0.000398	1.017387505	phosphatidylinositol glycan anchor biosynthesis, class A
MFSD1	0.002044	1.017059782	major facilitator superfamily domain containing 1
IL10	0.004629	1.016785699	interleukin 10
MYADM	0.010377	1.015394608	myeloid-associated differentiation marker
GRASP	0.014454	1.012612647	GRP1 (general receptor for phosphoinositides 1)-associated scaffold protein
CDC6	0.003893	1.011465962	cell division cycle 6
LOC100507217	0.001245	1.009227369	uncharacterized LOC100507217
USP38	0.010259	1.008764728	ubiquitin carboxyl-terminal hydrolase 38 isoform 2
EPN1	0.015742	1.007914098	epsin 1
GPR97	0.011842	1.007642903	G protein-coupled receptor 97
AZIN1	0.001377	1.00637416	antizyme inhibitor 1
SLC35E4	9.15E-05	1.004548891	solute carrier family 35, member E4

[a]Fold change ratio of expression in remission group to active group

Table S4. List of down-regulated genes in remission group with DESeq analysis

Gene symbol	Raw *P* value	R/A log2 fc[a]	Description
TAS2R4	3.25E-06	-1.93119111	taste receptor, type 2, member 4
KRT74	1.22E-06	-1.91868424	keratin 74
SPTSSB	4.89E-06	-1.840058846	serine palmitoyltransferase, small subunit B
CLDN24	1.12E-05	-1.833322418	claudin 24
DIP2A	3.53E-06	-1.676968833	DIP2 disco-interacting protein 2 homolog A (Drosophila)
LINC01355	5.70E-05	-1.661034058	
TDRKH	7.40E-05	-1.651506516	tudor and KH domain containing
C15orf54	1.98E-05	-1.553964197	chromosome 15 open reading frame 54
B3GALT2	0.000332	-1.481072951	UDP-Gal:betaGlcNAc beta 1,3-galactosyltransferase, polypeptide 2
GPR68	5.87E-05	-1.472377946	G protein-coupled receptor 68
COL5A3	0.000412	-1.420213197	collagen, type V, alpha 3
FAM150B	7.86E-05	-1.4063348	family with sequence similarity 150, member B
TNFSF4	0.000375	-1.401804021	tumor necrosis factor ligand superfamily member 4 isoform 2
S100B	0.000368	-1.368975465	S100 calcium binding protein B
KCNA5	0.001063	-1.365867699	potassium voltage-gated channel, shaker-related subfamily, member 5
ST3GAL6-AS1	0.001095	-1.351123145	ST3GAL6 antisense RNA 1
LOC100288842	0.000306	-1.323257659	UDP-GlcNAc:betaGal beta-1,3-N-acetylglucosaminyltransferase 5 pseudogene
OAS1	0.000407	-1.313353623	2′-5′-oligoadenylate synthetase 1, 40/46kDa
CLDN22	0.001501	-1.309912256	claudin 22
LINC00910	0.000753	-1.295237715	long intergenic non-protein coding RNA 910
LOC100272217	0.001916	-1.294850969	uncharacterized LOC100272217
KIF26B	0.000945	-1.287699277	kinesin family member 26B
RTKN2	0.001385	-1.280859548	rhotekin 2
RP11-166O4.5	0.002469	-1.256202713	uncharacterized LOC101929736
FDXR	0.00224	-1.255696436	ferredoxin reductase

LRRC26	0.002625	-1.255393639	leucine rich repeat containing 26
CCNJL	4.13E-05	-1.243946346	cyclin J-like
KIAA1161	0.001304	-1.231540352	KIAA1161
SLC25A20	1.76E-06	-1.225546391	solute carrier family 25 (carnitine/acylcarnitine translocase), member 20
LINC00469	0.003058	-1.219433409	long intergenic non-protein coding RNA 469
GPM6B	0.000379	-1.211191535	glycoprotein M6B
ZNF780B	0.000262	-1.192680516	zinc finger protein 780B
LOC102724297	0.002149	-1.192205271	
FLJ26850	0.004176	-1.187336405	FLJ26850 protein
PDE5A	0.004563	-1.179407293	phosphodiesterase 5A, cGMP-specific
LOC101927354	0.004593	-1.177332621	uncharacterized LOC101927354
VIPR2	0.000545	-1.171764032	vasoactive intestinal peptide receptor 2
CD160	0.000327	-1.170158516	CD160 molecule
LOC101929468	0.005197	-1.163632022	
IGIP	0.002688	-1.163188557	IgA-inducing protein
KLK14	0.002877	-1.162910231	kallikrein-related peptidase 14
EFNA5	0.002316	-1.160486381	ephrin-A5
TMEM155	0.001432	-1.158381085	transmembrane protein 155
MUC6	0.000327	-1.154017479	mucin 6, oligomeric mucus/gel-forming
BIN2	0.001338	-1.152130499	bridging integrator 2 isoform 4
CXCR3	0.005681	-1.150932985	chemokine (C-X-C motif) receptor 3
IFI44L	0.000176	-1.149267426	interferon-induced protein 44-like
AVPR1A	0.00229	-1.148389246	arginine vasopressin receptor 1A
WDR11-AS1	4.28E-05	-1.14672257	WDR11 antisense RNA 1
CD207	0.00312	-1.139657676	CD207 molecule, langerin
LRRC34	0.002643	-1.13909342	leucine rich repeat containing 34
MAD2L1BP	0.00648	-1.134996868	MAD2L1 binding protein
N6AMT1	0.003466	-1.127956634	N-6 adenine-specific DNA methyltransferase 1 (putative)
SLC25A19	0.006518	-1.125071101	solute carrier family 25 (mitochondrial thiamine pyrophosphate carrier), member 19
ZNF506	0.004149	-1.11932922	zinc finger protein 506
KCNIP2-AS1	0.000605	-1.118456006	KCNIP2 antisense RNA 1

ARMC2-AS1	0.007358	-1.116162419	ARMC2 antisense RNA 1
MORN1	0.007321	-1.113567924	MORN repeat-containing protein 1 isoform 2
CORO1B	0.004084	-1.112769029	coronin, actin binding protein, 1B
PI16	0.002597	-1.10802772	peptidase inhibitor 16
MAP3K7CL	0.000127	-1.100552037	MAP3K7 C-terminal like
LINC00861	0.001911	-1.097002029	long intergenic non-protein coding RNA 861
GAS1	0.005219	-1.094799584	growth arrest-specific 1
ENPP1	0.007233	-1.094381386	ectonucleotide pyrophosphatase /phosphodiesterase 1
CCDC7	5.47E-05	-1.08912484	coiled-coil domain containing 7
ITPR1-AS1	0.008514	-1.086824371	ITPR1 antisense RNA 1 (head to head)
LINC00563	0.008227	-1.080323861	long intergenic non-protein coding RNA 563
CA2	0.000364	-1.080137513	carbonic anhydrase II
CRYM-AS1	0.008124	-1.079378517	CRYM antisense RNA 1
CRIP2	0.009759	-1.078614017	cysteine-rich protein 2
ACTL10	0.00205	-1.075978339	actin-like 10
HYAL1	0.009385	-1.075584978	hyaluronoglucosaminidase 1
CHRNA5	0.009874	-1.071377367	cholinergic receptor, nicotinic, alpha 5 (neuronal)
LOC101927045	0.000513	-1.067610118	uncharacterized LOC101927045
SDCCAG3	0.005822	-1.066036749	serologically defined colon cancer antigen 3
XCL2	0.000609	-1.064954227	chemokine (C motif) ligand 2
PSPN	0.010421	-1.064366733	persephin
SLC35E2B	0.007979	-1.064291507	solute carrier family 35 member E2B
LOC400863	0.00527	-1.064218803	uncharactered LOC400863
RPS27A	0.010765	-1.064114777	ribosomal protein S27a
LINC00623	0.008865	-1.063920737	
TBCA	0.010862	-1.062601048	tubulin-specific chaperone A isoform 1
ZMAT4	0.005434	-1.062454371	zinc finger, matrin-type 4
RAB37	0.001026	-1.062226635	RAB37, member RAS oncogene family
TAS2R5	0.001183	-1.06164301	taste receptor, type 2, member 5
SLC10A5	0.005438	-1.061177745	solute carrier family 10, member 5
SLC3A1	0.000742	-1.058399235	solute carrier family 3 (amino acid transporter heavy chain), member 1
FAM178B	0.011056	-1.05729233	family with sequence similarity 178, member B
LINC00989	0.001971	-1.057156502	long intergenic non-protein coding RNA 989
LOC284648	0.009397	-1.056863289	uncharacterized LOC284648

GCSHP3	3.32E-05	-1.056194497	glycine cleavage system protein H (aminomethyl carrier) pseudogene 3
ARL6	0.011465	-1.054745334	ADP-ribosylation factor-like 6
PDE5A	0.001799	-1.054455794	phosphodiesterase 5A, cGMP-specific
EYA3	0.011396	-1.050573699	eyes absent homolog 3 (Drosophila)
TRHDE	0.009543	-1.048431482	thyrotropin-releasing hormone degrading enzyme
HOXA10-AS	0.000875	-1.047204398	HOXA10 antisense RNA
CD180	0.002807	-1.043403081	CD180 molecule
PARS2	0.011412	-1.04196241	prolyl-tRNA synthetase 2, mitochondrial (putative)
ALG1L9P	0.00257	-1.041775087	asparagine-linked glycosylation 1-like 9, pseudogene
UTS2	0.008432	-1.039353853	urotensin 2
LOC100128573	0.012568	-1.035506733	uncharacterized LOC100128573
ATL1	0.012932	-1.03445574	atlastin GTPase 1
ITGA10	3.93E-06	-1.034328384	integrin, alpha 10
HRH4	0.013027	-1.033485003	histamine receptor H4
ZNF658	0.002529	-1.033082284	zinc finger protein 658
C1orf186	0.000928	-1.032704352	chromosome 1 open reading frame 186
ADAMTS1	0.009475	-1.031543181	ADAM metallopeptidase with thrombospondin type 1 motif, 1
MAGI2-AS3	0.004975	-1.030837876	MAGI2 antisense RNA 3
ZSCAN32	0.010265	-1.028501486	zinc finger and SCAN domain containing 32
NKD1	0.001421	-1.028154574	naked cuticle homolog 1 (Drosophila)
HCG8	0.003459	-1.027573554	HLA complex group 8
HSD17B3	0.002273	-1.0272133	hydroxysteroid (17-beta) dehydrogenase 3
ZNF594	0.00529	-1.026663515	zinc finger protein 594
ZNF727	0.014002	-1.022854032	zinc finger protein 727
ATE1-AS1	0.011085	-1.022686523	
ARSK	1.20E-05	-1.01820499	arylsulfatase family, member K
PTENP1	0.003181	-1.015155968	phosphatase and tensin homolog pseudogene 1
LOC102723703	0.000166	-1.014501496	
RSAD2	0.000584	-1.014367646	radical S-adenosyl methionine domain containing 2
CNOT1	0.014875	-1.014190686	CCR4-NOT transcription complex, subunit 1
AC137932.6	0.003148	-1.013341709	uncharacterized LOC100287036
MANEA-AS1	0.011887	-1.008673737	MANEA antisense RNA 1 (head to head)

LINC00400	0.010466	-1.0078528	
BEND7	0.008256	-1.007513516	BEN domain containing 7
CCDC3	0.015837	-1.006768868	coiled-coil domain containing 3
FAM110C	0.010363	-1.006622913	family with sequence similarity 1 10, member C
LINC00665	0.015578	-1.005041861	long intergenic non-protein coding RNA 665

[a]Fold change ratio of expression in remission group to active group

요약 (국문초록)

배경 : 중증근무력증은 신경근접합부의 근막 구성 요소를 침범하는 자가면역성질환이다. 면역억제치료를 통해 질병의 관해가 이뤄지지만, 아직까지 그 기전이 어떻게 되는지 알지 못하며, 치료 반응을 추적할 수 있는 생체표지자 역시 밝혀져 있지 않다. 차세대염기서열분석이 가능해 짐에 따라 전체 리보핵산의 개요를 분석할 수 있게 되어, 본 연구에서는 중증근무력증 환자의 말초단핵구혈액세포에서 전사체 분석을 하여 질병 활성도와 관련된 분자적 특성을 규명하고자 한다.

방법 : 총 5명의 활성군 환자와 5명의 관해군 환자들에서 말초혈액단핵구세포를 추출하여 리보핵산 서열을 분석하였다. 활성군은 처음 진단되어 치료를 시작하기 전 상태이거나 치료 반응이 없는 환자들을 포함하였다. Cuffdiff와 DESeq을 이용하여 양 군간의 서로 다르게 발현된 유전자들을 분석하였으며, 이를 바탕으로 DAVID 및 IPA 프로그램을 이용하여 기능적 분석을 하였다.

결과 : Cuffdiff를 이용해 분석하였을 때 98개의 통계적으로 유의하게 차이가 나는 유전자가 관찰되었으며, 이 중 63개는 관해군에서 증가되어 있었고 35개는 감소되어 있었다. DESeq을 이용해 분석하였을 때에는 292개의 유전자가 유의하게 차이나는 것으로 관찰되었고, 이 중 28개가 두 가지 분석방법에서 공통적으로 관찰되고 있었다. 증가된 유전자 중 상위 5개는 PFKFB3, CTSG, RAB20, S100P, BEX1 이었고, 감소된 유전자 중 상위 5개는 S100B, OAS1, SLC25A20, MAP3K7CL, LINC00861 이었다. 기능적 분석에서는 세포이동과 관련된 유전자들의 변화가 나타났으며 이에 속하는 유전자들로는 ICAM1, CCL3, S100P, GAB2가 있었다. 또한 세포사멸과 관련된 유전자들의 변화도 나타났으며 NFKBIA, ZC3H12A, TNFAIP3, PPP1R15A 가 여기에 속하였다.

결론 : 본 연구에서는 중증근무력증의 질병 활성도에 따른 전사체와 그 기능적 군집의 발현량 차이를 분석하였다. 이 중 S100B, CXCR3이 관해군에서 감소되어 있었으며, 질환 활성도를 나타낼 수 있는 바이오마커로서의 가능성을 보였다. 기능적 분석에서는 세포이동 및 세포사멸과 관련된 경로가 양 군 간에 차이가 나타나 이와 관련된 유전자들을 후보 유전자로 사용하여 중증근무력증의 병리기전을 규명하기 위한 추가적 연구가 필요하다.

주요어 : 중증근무력증, 리보핵산염기서열분석, 전사체분석

학번 : 2010-21854